An Experimental Study of the Performance Characteristics with Four Different Rotor Blade Shapes on a Small Mixed-Type Turbine

Soo-Yong Cho*

Gyeongsang National University,
Department of Mechanical and Aerospace Engineering (ReCAPT),
Gajoadong 900, Jinju, Gyeongnam 660-701, Korea

Tae-Hwan Cho

Gyeongsang National University,
Department of Mechanical and Aerospace Engineering (ReCAPT),
Gajoadong 900, Jinju, Gyeongnam 660-701, Korea

Sang-Kyu Choi

Department of Advanced Industrial Technology,
Korea Institute of Material and Machinery,
Jangdong 171, Daejeon 305-343, Korea

A small mixed-type turbine with a diameter of 19.9 mm has been substituted for a rotational part of pencil-type air tool. Usually, a vane-type rotor is applied to the rotational part of the air tool. However, the vane-type rotor has some problems, such as friction, abrasion, and necessity of accurate assembly etc.,. These problems make the life time of the vane-type air tool short, but air tools operated by mixed-type turbines are free of friction and abrasion because the turbine rotor dose not contact with the casing. Moreover, it is assembled easily because of no axis offset. These characteristics are merits for using air tools, but loss of power is inevitable on a non-contacting type rotor due to flow loss, tip clearance loss, and profile loss etc.,. In this study, four different rotors are tested, and their characteristics are investigated by measuring the specific output power. Additionally, optimum nozzle location against the rotor is studied. Output powers are obtained through measured pressure, temperature, torque, rotational speed, and flow rate. The experimental results obtained with four different rotors show that the rotor blade shape greatly influences to the performance, and the optimum nozzle location exists near the mid span of the rotor.

Key Words : Mixed-Type Turbine, Rotor Blade Shape, Micro-Turbine, Air Tool, Turbine Performance

Nomenclature

a,b,c : Nozzle holes
Cj : Jet speed from nozzle

* Corresponding Author,
E-mail : sycho@gsnu.ac.kr
TEL : +82-55-751-6106; **FAX** : +82-55-757-5622
Gyeongsang National University, Department of Mechanical and Aerospace Engineering (ReCAPT), Gajoadong 900, Jinju, Gyeongnam 660-701, Korea. (Manuscript **Received** June 7, 2004; **Revised** June 13, 2005)

F : Operating force, g_f
H : Output power, Watts
h : Specific output power, Watts/(g/sec)
$\dot{m}$: Mass flow rate, g/sec
$P_{in,rel}$: Total inlet gauge pressure at rotor inlet, kPa
Q : Flow rate, l/min
$T_{in,st}$: Static inlet absolute temperature at rotor inlet, K

T_{std} : Absolute temperature at sea level, K
U : Blade speed

Greek Symbols

ϑ : Temperature corrected parameter, $T_{in,st}/T_{std}$

$\varPi$: Net specific output power, (Watts.rad)/sec

Ω : Rotational speed, RPM

ω : Rotational speed, rad/sec

1. Introduction

Air tools with a casing diameter less than 30mm are classified as pencil-type. They are used for removing burrs on the edge of workpieces or castings, shaping surface of dies, and polishing of materials such as steel, wood and ceramic etc.,. Generally, vane-type rotors are adopted as a rotating driver as shown in Fig. 1, but the vane-type rotor has some problems such as friction between the vane and cylinder block, abrasion on the vane tip and inner surface of the cylinder block, and the need for accurate assembly due to axis offset between the rotor and the cylinder. In order to solve these problems, a turbine rotor could be applied to the rotating driver because it operates without any frictional force. However, the turbine rotor should be maintained at a diameter of less than 20 mm, and should be operated with partial admission because the flow rate should not be increased by changing the rotor type. Some researches about the partial admission have been conducted in order to obtain high specific power in a state of low specific speed.
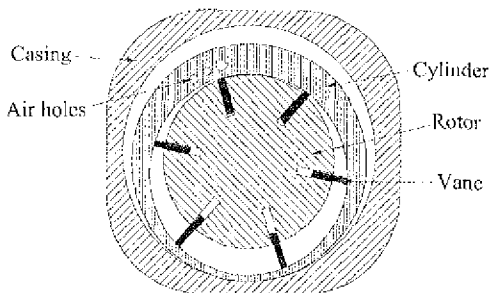

Fig. 1 Cross sectional view of the rotor used in a vane-type air tool

Robert et al.(1949) showed experimental results that the output power of a gas turbine quickly decreased when the partial admission area on the nozzle was reduced to more than half of the full admission area. Balje and Binsley (1969) showed additional losses by the partial admission such as filling and emptying loss, scavenge loss, blade pumping loss, and tip clearance loss. Boulbin et al.(1994) showed that the operating force on a rotor depended on the relative location of the rotor blade in the partial admission region. They showed that the operating force decreased when the rotor entered into the partial admission region. However, the operating force quickly increased when the rotor entered into the arc of admission fully, and a peak force was obtained at exit of the arc of admission. He (1997) showed that efficiency on a turbine operated with partial admission was influenced by the non-uniform flow along the circumference. In a multi stage machine, an effect of the non-uniform flow was insignificant after the first stage because the non-uniformity of flow was quickly decayed. Bohn et al.(1998) showed a variation of efficiency by changing the shape of cross-over channel and the flow rate. The efficiency depended on the shape of cross-over channel in the full admission state, but in the partial admission state, it was much more dependant on the flow rate than the shape of cross-over channel. Skopek et al.(1999) investigated variations of efficiency by reducing the partial admission flow rate to 0.4. They showed that the efficiency was increased by reducing the axial gap between nozzle and rotor. When the flow rate was reduced, the efficiency and optimum velocity ratio (U/C_j) were decreased.

Even though these results were obtained on axial-type machines with the partial admission, these do offer an important physical phenomenon such as the efficiency and the optimum velocity ratio are decreased when the admission rate is reduced. In order to apply the partial admission to an air tool efficiently, one needs to understand characteristics of the rotor blade on a turbine type air tool to obtain high torque through minimizing the partial admission area. In this study,

performance of various mixed type rotor blades is therefore investigated experimentally with the partial admission.

2. Rotor Blade Profile and Apparatus

2.1 Mixed type rotor

Even though an air tool using a turbine for the rotating part has great merit such that it operates in a non-contacting state, its manufacturing cost depends on a certain type of turbine rotor. If an axial-type turbine rotor is adopted, manufacturing costs increase due to the multi stage and a complicated blade shape. To avoid this problem, a mixed-type turbine rotor could be adopted because the rotor can be easily manufactured through die casting. Usually, characteristics of a turbine rotor are different from those of a vane-type rotor because the turbine rotor operates in a non-contacting state. On the vane-type rotor, the operating force depends on the flow rate and operating air pressure, but on the turbine rotor, the operating force is changed with the flow angle and shape of rotor blade as well as the flow rate and operating air pressure.

Figure 2 shows the structure of a mixed-type air tool applied in this study. Three nozzles are installed along the axial direction, and these are installed symmetrically at 180° on the circumference respectively. Six nozzles are therefore applied in this experiment. The jet flow angle from the nozzle is a 80° from the radial direction and also is maintained a 60° from the axial direction. So, high pressure air is impinged onto the rotor blade at an axially and circumferentially tilted direction. The axial gap between each nozzle is 5 mm, and the axial length from the rotor hub to the first nozzle is 1.5 mm. Figure 3 shows four different rotor blade profiles, which are obtained on the cross section against the rotor axis shown in the structure of Fig. 2. Each blade profile is a camber of the rotor blade, which has a 1.5 mm thickness.

On an air tool using turbine rotor, the flow passage should be designed so that the rotor can obtain a greater reaction force because the turbine

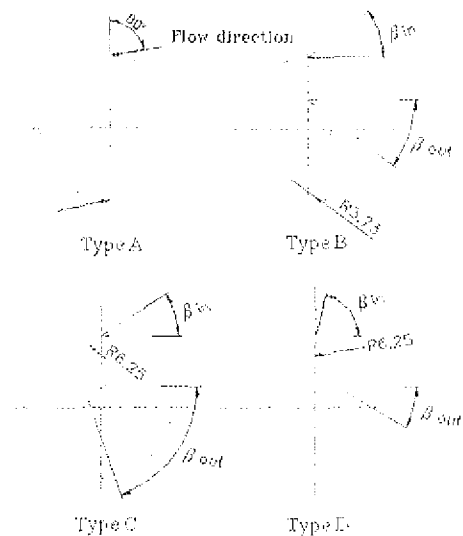**Fig. 2** Structure drawing of air tool using a mixed type turbine rotor

Fig. 3 Various rotor blade shapes at the hub and flow direction

rotor gets the output power from the impulse force. This impulse force is decided from the flow angle at inlet and exit, which is affected by the shape of the rotor blade. It is therefore directly related to the output power on the air tool using turbine rotors. Cho et al. (2002) showed how to improve a rotor blade's shape using an optimization with blade design variables for increasing the output power. Table 1 shows the blade angle at inlet and exit, its radius and incidence. The blade angle is defined at an angle between the horizontal line and the blade line at inlet and exit as shown in Fig. 2. In case of type A blades, the chord is 6 mm at the hub and the blade profile is linear. Type B blades have the same blade angle at inlet and exit. The center of circle on type C and D blade is (3.33, 4.66) and (6.02, 8.26) based on the axis, respectively. The incidence is ob-

Table 1 Dimension of rotor blade profiles

Rotor Blade	Inlet Angle (β_{in})	Outlet Angle (β_{out})	Radius (mm)	Incidence
Type A	–	–	–	78.6°
Type B	37°	37°	3.73	25.6°
Type C	32.2°	74.3°	6.25	21.1°
Type D	74.3°	30°	6.25	62.9°

tained from the angle between the relative flow angle and blade inlet angle.

2.2 Experimental apparatus

Performance of rotating machinery could be evaluated when the operating torque and air properties are measured in a rotating status. However, it is hard to test a low power turbine because it operates in a status of low torque at high RPM, such as a 20 N.mm at a 50,000 RPM range. This operating condition therefore makes it hard to apply commercial torque sensors. For examples, a slip ring type torque sensor for measuring the lowest torque in products of Lebow (1998) can measure only 70 N.mm at a maximum of 20,000 RPM. In case of a transformer type torque sensor, 350 N.mm at a 20,000 RPM is the lowest measurable torque.

Another applicable commercial torque meter could be small dynamometers which are produced at Megtrol (2004). Among them, the lowest measurable torque in a rotating state is 18 N.mm at a maximum of 30,000 RPM. This dynamometer therefore could not be applied to the test of a small turbine because the operating RPM is higher than the maximum RPM of the dynamometer. If a reduction gear is installed between the axis of the turbine and dynamometer to reduce input RPM, this dynamometer could then be applied to tests of high RPM machines. However, test results obtained from the dynamometer with a reduction gear showed 50% lower output power than those obtained from a frictional type torque meter in a test for a small axial type turbine (Cho and Kim, 2003). This is caused by power losses on the reduction gear and added mass on the rotating part of the turbine because the dynamometer uses an eddy current type brak-

Table 2 Degree of accuracy for measuring instruments applied to experimental apparatus

Measuring Instruments	Models	Accuracy
Flowmeter	HFM201 Hastings Instruments	Less than 0.5% @ %FS
Loadcell	34/1944-07 Sensotec	±0.02% Max. 250gf
RPM Gauge	ACT-3 Monarch	±0.0015% Max. 100,000RPM
Pressure Gauge	811 FMG Sensotec	Less than 0.25% @ %FS
DAQ	NI 6014	200kS/sec

ing system. In order to avoid these losses, a frictional type torque meter is applied to this experiment.

A cone shape is applied to minimize vibration caused by the frictional force. Moreover, this shape makes setting up the turbine easily with accurate eccentricity and alignment to the torque meter. The surface was heat treated after grinding so as not to cause vibration through the abrasion. The frictional type RPM controller is supported using two ball bearings to minimize the frictional force along the circumferential direction and its housing is installed on a movable vise. A support device of turbine is installed on a 3 dimensional traverse to adjust the axis of
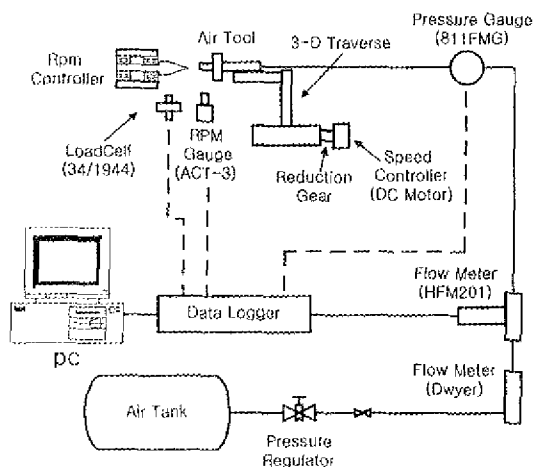
Fig. 4 Schematic diagram of experimental apparatus

the turbine accurately. A reduction gear with DC
motor is used to control the frictional force by
adjusting the traverse speed of the turbine. This
makes it so that the frictional force increases
smoothly and the operating RPM decreases con-
tinuously. Operating forces of the turbine are
measured using a loadcell of which the end is
connected using a wire with a point located on
the cone shaft of which the radius is 8.75 mm.
Figure 4 shows a schematic diagram of this ex-
perimental apparatus. Table 2 shows the accuracy
of the measuring instruments.

3. Results and Discussions

Specific output power (h) obtained using vari-
ous rotors is shown in Fig. 5 with RPM and mass
flow rate change. The RPM (Ω) compensated
with the temperature corrected parameter (ϑ) is
shown in the abscissa. The specific output power
is obtained from the output power divided by the
mass flow rate as Eq. (1).

$$h = \frac{H}{\dot{m}} = \frac{F * 0.875 * \Omega}{1000 * 97.4 * \dot{m}} \qquad (1)$$

where F is the operating force of the turbine. In
order to change the mass flow rate, several inner
cases are manufactured with different nozzle di-
ameter. If the mass flow rate is changed using a
valve on the high pressure air supply line instead
of the nozzle diameter, the inlet pressure could
not be maintained at a constant when the mass
flow rate changes. In this experiment, the inlet
pressure therefore was maintained at a constant
because the mass flow rate was adjusted by the
nozzle area.

The specific output power increases with in-
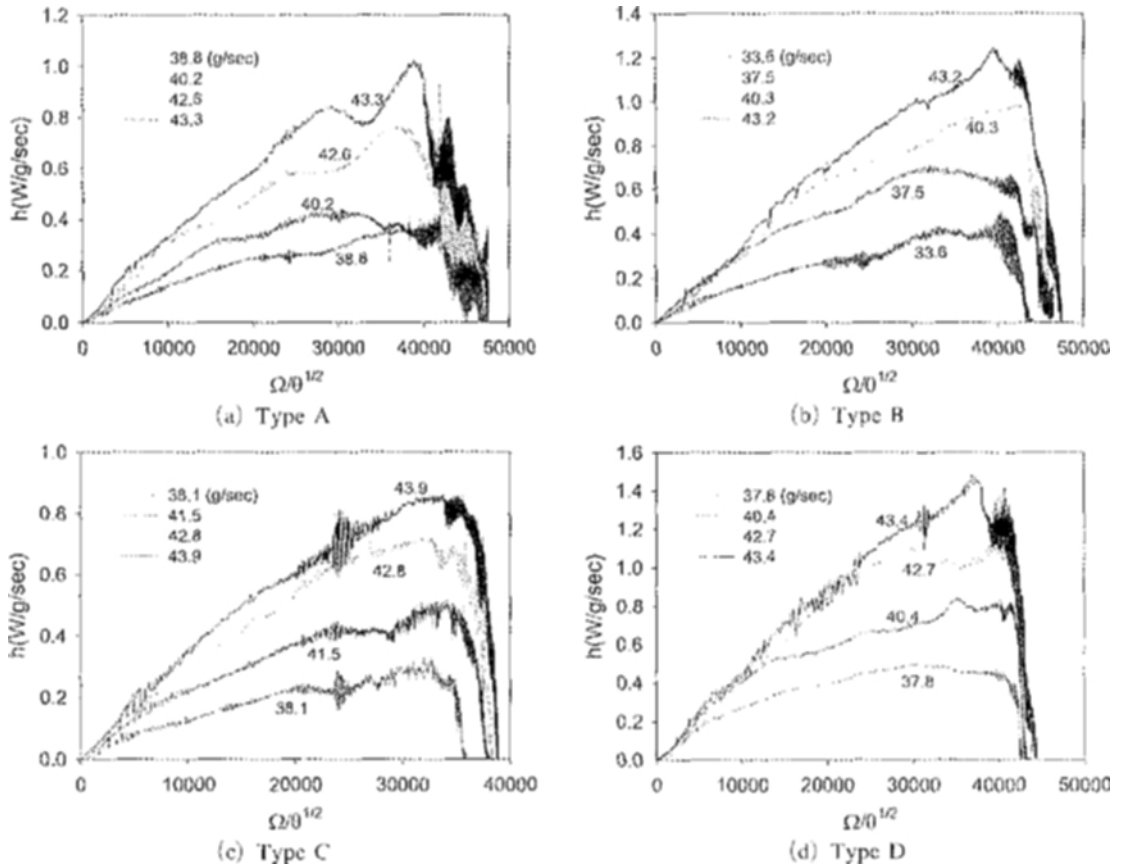creasing the mass flow rate as shown in Fig. 5.

(a) Type A

(b) Type B

(c) Type C

(d) Type D

Fig. 5 Specific output power with various rotor blade types

These characteristics occur on the turbine operating with partial admission. In a partial admission, turbine efficiency and optimum velocity ratio (U/Cj) are quickly decreased when the mass flow rate is reduced, so high efficiency is obtained by increasing the mass flow rate at the same RPM condition. However, the increment of mass flow rate increases the operating cost. A turbine rotor should therefore be designed to obtain the high specific power with a low mass flow rate.

Curves of the specific output power for the RPM show a similar trend even though the shape of rotors is changed. The reason is that radial or mixed-type rotors have general characteristics such as the operating torque quickly increases when the frictional force is loaded at the unloaded rotational speed. In case of type A rotor, unstable situations such as an operation at a critical speed are shown in the high rotational

speed region of 45,000 RPM, but the type C rotor shows this unstable operation in the mid rotational speed region of 25,000 RPM. The type B rotor and D rotor show that the specific output power is changed smoothly in the whole rotational speed region. Only at the peak region of the specific output power, they show a slightly unstable situation due to the characteristics of the radial or mixed-type turbine. After passing this region, they show that the specific output power is decreased linearly as the frictional force is increased.
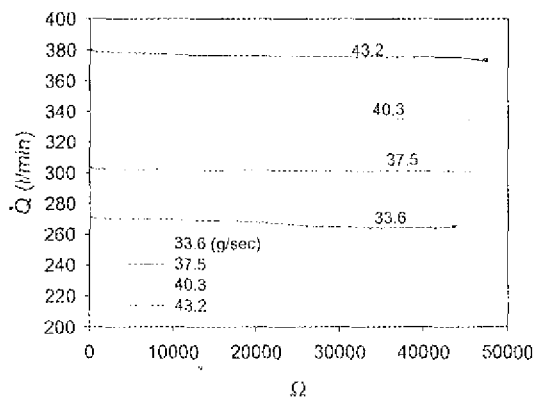
These results show that a region for the highest specific output power exists in a 15-20% lower rotational speed than the unloaded rotational speed, and this region is slightly changed when the mass flow rate is varied. The best performance is therefore obtained when the turbine operates in this rotational speed region.
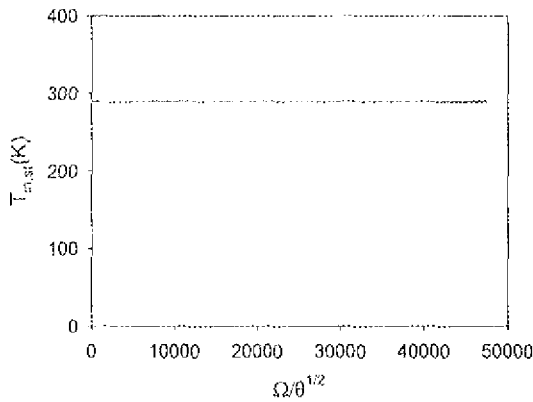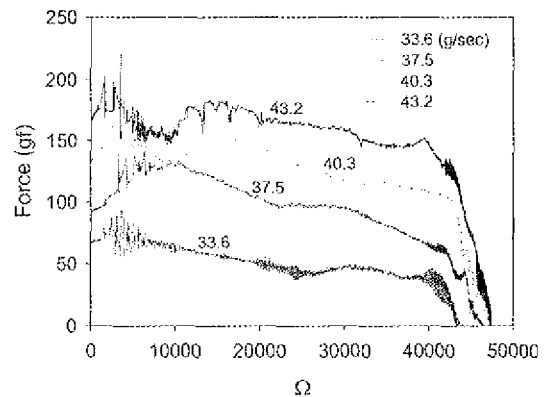

(a) Inlet temperature
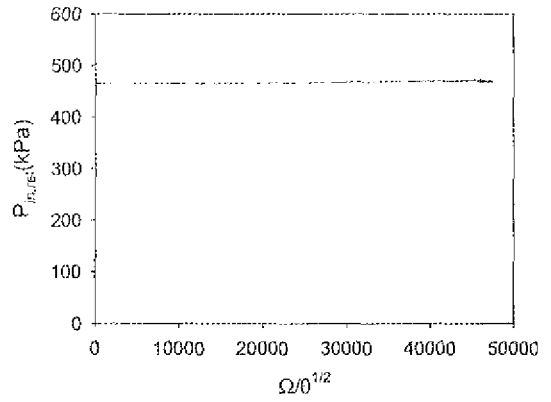
(b) Inlet pressure

(c) Volume flow rate

(d) Operating force

Fig. 6 Inlet conditions and operating status on Type B rotor

Inlet conditions and operating forces on the type B rotor which exhibits the best performance among the 4 different rotors are shown in Fig. 6. Figure 6(a) (b) show that the inlet gauge pressure and static temperature do not change during operation. The reason is that the nozzle inlet state becomes like a reservoir's state due to the very small nozzle area. This makes so that the inlet condition does not change with the rotational speed. Additionally, the flow rate is also maintained at a constant during operation as shown in Fig. 6(c) because the flow rate is changed only in the nozzle area and the flow at the nozzle is chocked. Figure 6(d) shows the operating force with RPM change when the mass flow rate is fixed. The operating force is quickly increased when the frictional force is loaded at the unloaded rotational speed, and then it is increased smoothly with decreasing RPM as the frictional force is increased. The highest operating force is obtained at very low RPM. After the RPM obtained the peak operating force, the operating force is quickly dropped to a lower force which can be maintained even though the rotational speed is zero. The magnitude of this force depends on the shape of the rotor blade.

Small turbine needs not only high rotational speed but also high operating torque to be applied as an air tool rotor. The high rotational speed has an advantage for cutting or grinding effectively, and the high operating torque gives a good working performance. In comparison with the performance of small turbine, the specific output power could usually be applied, but this specific output power is used only at a fixed rotational speed. Data of specific output power are therefore not enough to use for comparing the overall performance of small turbine, i.e. when the rotational speed is decreased, the specific output power is also decreased but the operating torque is increased. In order to consider the specific output power effect and the operating torque effect together, a net specific output power should be calculated. The net specific output power is obtained by integrating the specific output power with the rotational speed as Eq. (2).
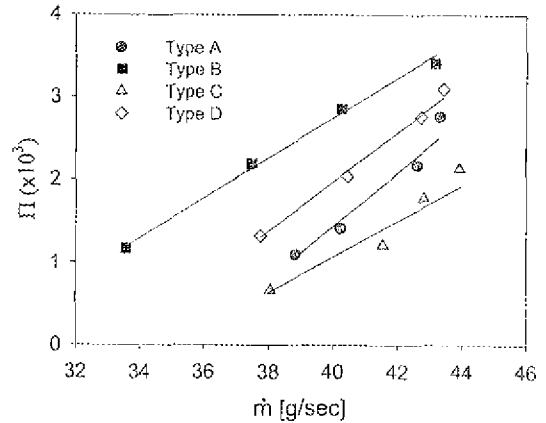

Fig. 7 Net specific output power on various rotor types when mass flow rate is changed

$$H = \int h \, d\omega \qquad (2)$$

where h is the specific output power and ω means the rotational speed.

Figure 7 shows variations of the net specific output power for four different rotor blades when the mass flow rate varies. The highest net specific output power is obtained when the type B rotor is applied, and the type D rotor shows the second best performance among the four rotor blades. In the case of the type D rotor, it was designed with two and half times bigger incidence than that of the type B rotor to increase the reaction force. However, experimental results show that this big incidence causes an incidence loss at the rotor inlet. This loss affects the net specific output power, and so to increase the net specific output power, the incidence and the inlet flow angle should be selected appropriately.

In order to investigate the effect of the incidence and the reaction force to the net specific output power, a type C rotor blade is designed in order to get smaller incidence than the type D rotor. The incidence on the type C rotor is selected as an angle which is recommended on the standard blade. However, the net specific output power obtained using the type C rotor is worse than that using the type D rotor. These experimental results show that the reaction force is more important than the incidence angle in the partial admission. The type A rotor blade is designed as straight

type, which is easier to manufacture than others. However, the experimental result show that the net specific output powers obtained using the type A rotor are better than those with the type C rotor, and worse than those with the type D rotor. What the performance of type A rotor is worse than that of type D rotor is easily acceptable because the type A rotor blade has a 16° bigger incidence and larger exit blade angle than those of type D rotor blades. Comparing with the type A and C rotor, the type A rotor obtains more reaction force even though incidence loss is bigger than that of the type C rotor. This result is consistent with the experimental results obtained with the type B, C and D rotors.

As shown in Fig. 2, the rotor has long blades along the axial direction. So, the output power is affected by the location of the nozzle. Figure 8 shows the difference of the net specific output power when nozzles on different location are used. The abscissa in Fig. 8 means the location of the nozzle. Nozzle (a) is located near the hub, while nozzle (b) is the second along the axial direction, and finally nozzle (c) is located near the tip. Each nozzle spouts high pressure air into the rotor symmetrically. The net specific output power obtained with all nozzles such as (a+b+c) shows the same experimental result as shown in Fig. 7. In the experimental result with each nozzle, the highest net specific output power is obtained with nozzle (b) which is located in the
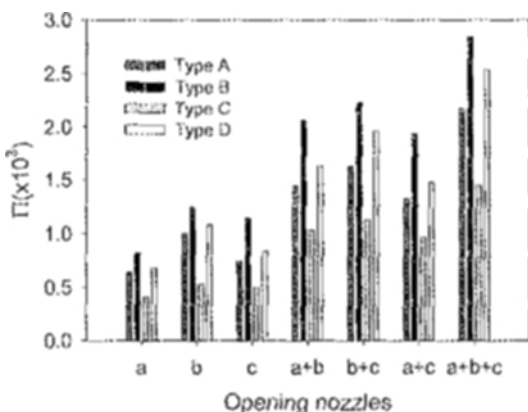
mid of the rotor blade and the worst one is obtained with nozzle (a) which is located near the hub. The worst result shown by nozzle (a) comes from the pumping effect due to the long blade.

In the experimental results conducted after selecting two nozzles among three, the highest net specific output power is obtained when nozzle (b) and nozzle (c) are used simultaneously. When nozzle (a) and nozzle (c) are applied, the net specific output power is the worst. These results are consistent with the experimental results obtained with each nozzle, and also the net specific output power with different axial nozzle location is independent on the shape of the rotor blade. This means that nozzles prefer to be installed circumferentially instead of in an axial direction to obtain the net specific output power
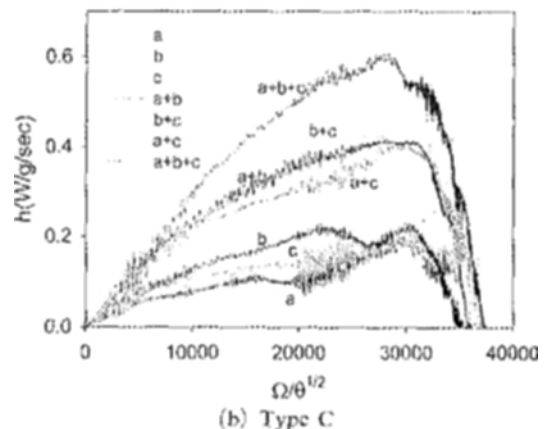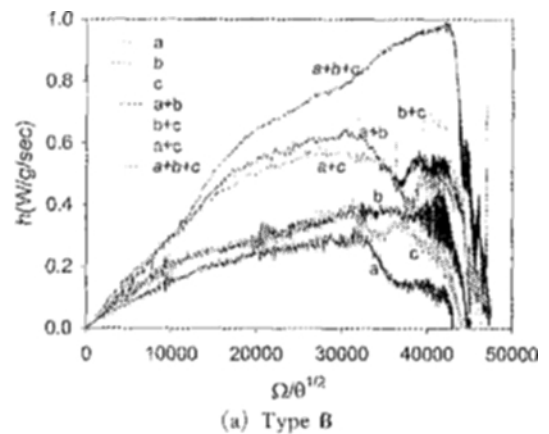

(a) Type B

Fig. 8 Net specific output power on various rotor types when operating nozzles are chosen

(b) Type C

Fig. 9 Specific output power on the type B and C rotor when operating nozzles are chosen

Soo-Yong Cho, Tae-Hwan Cho and Sang-Kyu Choi

efficiently. In case of the long blade air tool, it would be better to install nozzle (a) and nozzle (c) circumferentially with nozzle (b) at the mid location of the rotor blade.

Figure 9 shows the specific output power on the type B and C rotors according to the different nozzle locations, with the applied nozzle diameter being 1mm. Two experimental results show similar phenomena such as the specific output power is quickly increased at the high rotational speed and then smoothly decreased by diminishing the rotational speed after passing the peak value. The variation of the specific output power is very similar with the results shown in Fig. 5. This means that the specific output power obtained with different nozzles has a similar trend as the specific output power obtained with different mass flow rates.

4. Conclusions

A performance test is conducted on a small mixed-type turbine of which the rotor has four different rotor blades. The net specific output power and the specific output power are measured with different rotor blades and nozzle locations.

(1) In order to obtain more output power with given constant mass flow rate, the shape of the rotor blade should be designed to generate more reaction force because the reaction force has a more effective factor for the output power than that of incidence loss if the incidence does not have a big discrepancy from the standard incidence.

(2) The highest specific output power is obtained at a 15-20% lower rotational speed than the maximum rotational speed, while this rotational speed for the highest specific output power is slightly decreased when the mass flow rate is decreased.

(3) In the long blade and mixed type turbine, the nozzle located in the mid of the rotor blade shows the best performance. It would be preferred for better performance to install the nozzle circumferentially instead of installing the nozzle along the axial direction.

References

Balje, O. E. and Binsley, R. L., 1968, "Axial Turbine Performance Evaluation Part A – Loss Geometry Relationships," *J. of Eng. for Power*, pp. 341~348.

Bohn, D., Drexler, Chr. and Emunds, R., 1993, "Experimental and Theoretical Investigations into the Non-uniform Flow of a Partial Admission Turbine with a Multistage Blading," *VGB Kraftwerkstechnik* 73, No. 8, pp. 610~608.

Bohn, D., Gier, J. and Ziemann, M., 1998, "Influence of the Cross-Over Channel Geometry on the Flow Equalization in Partial-Admission Turbines," *VGB PowerTech* 2, pp. 49~54.

Boulbin, F., Hetet, J. F. and Chesse, P., 1994, "Non-steady Flow in the Partial Admission," *VDI Berichte NR*, 1109, pp. 395~401.

Cho, S. Y. and Kim, E. S., 2003, "Study on Measuring the Performance of an Air Tool Operating at 100,000RPM Class," *J. of Fluid Machinery*, Vol. 6, No. 3, pp. 44~50.

Cho, S. Y., Yoon, E. S. and Choi, B. S., 2002, "A Study on an Axial-Type 2-D Turbine Blade Shape for Reducing the Blade Profile Loss," *KSME int. J.*, Vol. 16, No. 8, pp. 1154~1164. (in Korea)

He, L., 1997, "Computation of Unsteady Flow Through Steam Turbine Blade Row at Partial Admission," *Proc. Instit. Mech. Engrs.*, Vol. 211 Part A, pp. 197~205.

Lebow, 1998, "Load Cell and Torque Sensor Handbook No. 710B," Lebow Products, Troy, Michigan, USA.

Magtrol, 2004, "Product User's Manuals," 2000-2004 Magtrol, Inc., 74M124, USA.

Robert, C. K., Howard, Z. H. and Warren, J. W., 1949, "Effects of Partial Admission on Per-

formance of a Gas Turbine," *NACA Technical Note* No.1807.

Skopec, J., Vomela, L., Tajc, L. and Polansky, J., 1999, "Partial Steam Admission in an Axial Turbine Stage," *IMechE Conference Transactions*, 1999, Third European Conference on Turbomachinery, Vol. B C557/077/99, pp. 681~691.